2021 43rd Annual International Conference of the
IEEE Engineering in Medicine & Biology Society (EMBC)
Oct 31 - Nov 4, 2021. Virtual Conference

Automatic Multi-Atlas Liver Segmentation and Couinaud Classification from CT Volumes

Sofia Pla-Alemany, Juan Antonio Romero, José Manuel Santabárbara,
Roberto Aliaga, Alicia M. Maceira, and David Moratal, *Senior Member, IEEE*

***Abstract*— Primary Live Cancer (PLC) is the sixth most common cancer worldwide and its occurrence predominates in patients with chronic liver diseases and other risk factors like hepatitis B and C. Treatment of PLC and malignant liver tumors depend both in tumor characteristics and the functional status of the organ, thus must be individualized for each patient. Liver segmentation and classification according to Couinaud's classification is essential for computer-aided diagnosis and treatment planning, however, manual segmentation of the liver volume slice by slice can be a time-consuming and challenging task and it is highly dependent on the experience of the user. We propose an alternative automatic segmentation method that allows accuracy and time consumption amelioration. The procedure pursues a multi-atlas based classification for Couinaud segmentation. Our algorithm was implemented on 20 subjects from the IRCAD 3D data base in order to segment and classify the liver volume in its Couinaud segments, obtaining an average DICE coefficient of 0.94.**

***Clinical Relevance*— The final purpose of this work is to provide an automatic multi-atlas liver segmentation and Couinaud classification by means of CT image analysis.**

I. Introduction

Primary Liver Cancer (PLC) is the sixth most common cancer worldwide, its incidence is increasing worldwide [1] and its occurrence predominates in patients with chronic liver disease and other risks factors, such as viral hepatitis B and C. Treatment of PLC and malignant liver tumors depend both in tumor characteristics and the functional status of the organ, thus should be individualized for each patient.

Several treatment approaches are often considered, including ablation for small tumors, liver resection or liver transplantation. Although liver resections are often challenging due to its complex anatomy, the role of hepatectomies for liver tumor treatment is expanding and improving patient outcomes due to advances on surgical resections in recent years [2]. According to Couinaud [3] the liver is functionally divided into eight segments defined by portal and hepatic veins. This partition allows resection surgeries of one or more pathological segments while preserving the blood flow of healthy tissue.

Medical imaging techniques, such as contrast enhanced Computed Tomography (CT), are essential for the detection of hepatic regions and vascular structures that allow physicians to make a proper decision and preoperative planning of resection treatment [4]. Automatic segmentation of 3D CT images of the liver via computer-aided diagnostic and treatment planning tools are the first step to describe the pathological and anatomical structures of the liver [5,6]. Nevertheless, the liver is one of the most difficult organs to segment as it presents challenges such as high shape and intensity variability between subjects and proximity to organs with similar intensities [7,8].

Existing strategies are divided into two types: data-based, and model-based methods [4]. Data-based strategies depend on image histogram and include region growing [9],[10] active contours [11] or graph cut [12] methods. The latter are fast but lack spatial information and often result on unsuccessful demarcation of boundaries, requiring user correction. They are therefore commonly combined with model-based methods such as atlas-based segmentation [13] or statistical shape models [14], which work with prior information about shape and location of anatomical structures to overcome the proximity of organs with similar intensities [15]. However, atlas or statistical model construction are complex and prior templates with high anatomical variability are not always available.

This paper presents an automatic segmentation method of the liver based on the Couinaud scheme from contrast enhanced CT images. Specifically, we have opted for a multi-atlas-based (MAS) and a single-atlas-based segmentation strategy for liver boundary detection and Couinaud classification, respectively. Our method was tested in clinical data publicly available in 3D-IRCAD data base (www.ircad.fr).

II. Material and Methods

A. Atlas and Subjects

Twenty subjects from the publicly available 3D-IRCAD 01 data base, which include 20 challenging cases for segmentation with high variability in tumor number and size, were employed for testing. The 3D CT scans slice thickness

Corresponding author: David Moratal (e-mail: dmoratal@eln.upv.es).

The authors acknowledge financial support from the "Conselleria d'Educació, Investigació, Cultura i Esport, Generalitat Valenciana" (grants AEST/2019/037 and AEST/2020/029), from the "Agencia Valenciana de la Innovación, Generalitat Valenciana" (ref. INNCAD00/19/085 and INNCAD/2020/84), and from the "Centro para el Desarrollo Tecnológico Industrial" (Programa Eurostars-2, actuación Interempresas Internacional), Spanish "Ministerio de Ciencia, Innovación y Universidades" (ref. CIIP-20192020).

S. Pla-Alemany and D. Moratal are with Center for Biomaterials and Tissue Engineering, Universitat Politècnica de València, Spain.

J. A. Romero, J. M. Santabárbara, R. Aliaga, and A. M. Maceira are with ASCIRES Biomedical Group, Valencia, Spain.

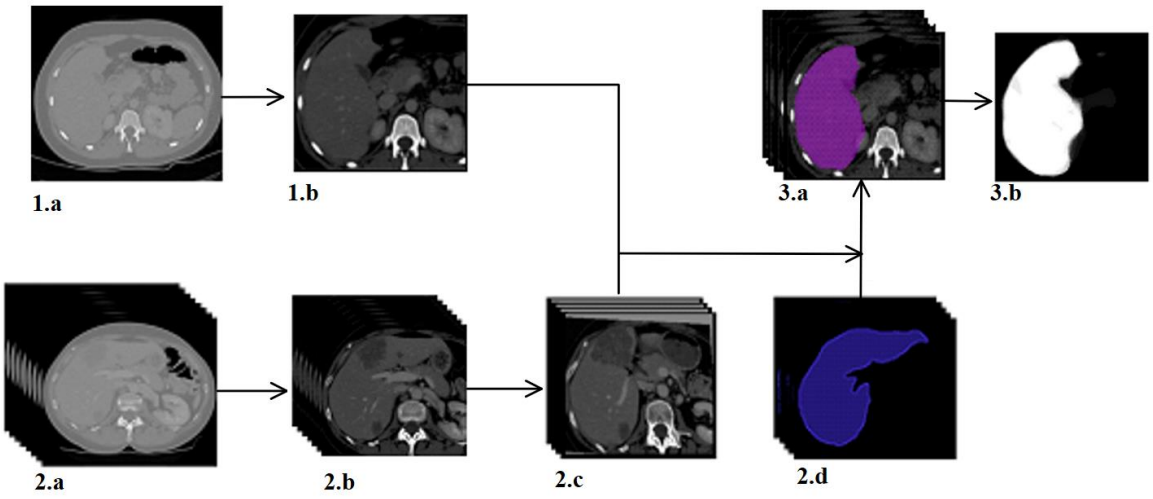

Fig. 1. Workflow proposed in method. (1.a) Computed Tomography slice of a novel image. (1.b) Slice of preprocessed novel image. (2.a) Set of 20 IRCAD atlases. (2.b) Set of 20 preprocessed atlases. (2.c) Selected atlases. (2.d) Liver labels of selected atlas. (3.a) Propagated labels from selected atlases. (3.b) Probability map result of label fusion.

and resolution of such data base subjects varies between 1.0 to 4.0 mm and from 0.56 mm^2 to 0.81 mm^2 respectively. A leave-one-out based study was conducted so each of the 20 subjects CT scans where segmented via the MAS technique while the other 19 CT scans and respective ground truths were employed as the atlases providing prior information.

To evaluate and validate our developed method, the results were compared to the ground truth by means of the DICE coefficient [16] (1), percentage value error (PVE) (2) false positive (FP) and false negative (FN) rates.

The DICE coefficient and PVE are defined as:

$$DICE = 2 * \frac{|X \cap Y|}{|X|+|Y|} \quad (1)$$

$$PVE = \frac{X-Y}{Y} * 100\% \quad (2)$$

where,
X is the liver volume segmented by our algorithm
Y is the ground truth liver volume segmented manually.

Furthermore, the Surgical Planning Laboratory (SPL) Liver atlas was used. It is publicly available in the Open Anatomy Project platform and includes one 3D CT scan including the Couinaud segments labels that provide prior information needed for Couinaud single-atlas-based classification of liver volume.

B. Multi-atlas based Segmentation

Multi-atlas segmentation relies on the existence of multiple reference images (i.e. atlases) where the object of interest has been previously segmented. This allows finding a point-to-point spatial correspondence of the atlases and the novel image via image registration. A transformation is computed and then used to deform the atlases binary masks obtaining candidate segmentations for the novel image.

The proposed method follows the workflow depicted in Fig.1 and described in Fig. 2. and it establishes the spatial correlations between 20 atlases and the novel image to subsequently combine the resulting deformed binary mask to obtain the final segmentation.

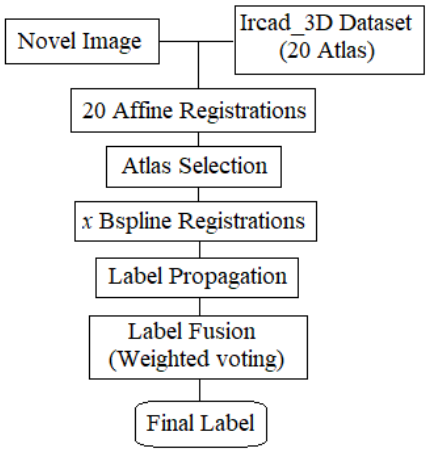

Fig. 2 Liver atlas-based segmentation workflow

1) Affine Registration

Image registration is an iterative process that involves the deformation of an image to maximize an objective function with respect to a spatial alignment metric. The main components are thus the deformation model, the objective function, and the optimizer. An affine registration is the first step of our algorithm. It is performed by means of the open source software *Elastix* [17] and it results on a linear deformation model with twelve degrees of freedom using normalized mutual information (NMI) metric and two resolution levels.

2) Atlas Selection

There are two main motivations not to use all the available atlases. In the first place, image registration involves high computational cost, in fact, computational efficiency of MAS algorithms is linear to the number of selected atlases [18].

Therefore, an optimal selection of atlases can increase speed, reduce memory consumption, and exclude irrelevant atlases that might misguide the segmentation process. In this work, a compromise between a well-informed selection step and an optimal computational cost is achieved by linearly registering all the atlases to the novel image. This allows ranking the relevance of each atlas to perform an informed atlas selection. The similarity measure employed to evaluate atlas similarity with novel image was NMI, thus, atlases with an NMI higher than the median are selected.

3) B-spline Registration

Once the most reliable atlases have been selected, the method proceeds with the definition of the spatial correlation between the selected atlases and the novel image. A nonlinear spline-based method is employed, where B-splines are placed on a regular grid to assign a spatial transformation vector to each control point, seeking voxel-label alignment accuracy. The objective function is again based on NMI, and the optimizer and three resolutions are employed

4) Label Propagation

In MAS algorithms, the nonlinear deformation between both images is computed with the final purpose of propagating the atlas label. Therefore, once spatial correspondences have been established with the novel image, the geometrical transforms obtained for each atlas are applied to their respective liver label, step known as label propagation. As a result, we obtain the same number of liver binary mask candidates as selected atlases.

5) Label fusion

Label fusion is conducted sequentially by combining the propagated labels by means of weighted voting. Each candidate label obtained from label propagation is associated with a weight that reflects the similarity between the registered atlas and the novel image, proportional to the final NMI metric value for non-lineal registration. Weighted voting results on a probability map, where the value of each pixel indicates its probability of belonging to liver tissue. Finally, a probability threshold is defined to determine which pixels finally belong to the livers mask. For this study, a default value is set at 0.8, however, the user can easily choose to modify this threshold if this can improve the accuracy of the final segmentation.

C. Single-Atlas Based Couinaud Classification

The Couinaud scheme divides the liver into eight independent segments, each one having their own independent vascular and biliary drainage. This anatomic division allows save resections of individual segments without damaging the healthy remaining segments. This algorithm employs the previously segmented liver volume and atlas-based prior information from SPL atlas for the process of Couinaud segments classification.

The first step of this process is the affine registration, subsequently followed by the spline-based registration of the liver binary mask previously obtained and the SPL atlas binary mask. Once the deformation between both masks is defined, Couinaud labels are propagated, resulting on a first approximation of the Couinaud scheme for the novel image. As a result, the liver volume will be divided into an upper portion, comprised by segments II, IVa, V, VIII, and a lower portion comprised by segments III, IVb, VI and VII, together with segment I on the posterior face. This process follows a single atlas-based strategy given the lack of available atlas including Couinaud labels.

III. RESULTS

Table 1 shows the segmentation results of the 20 data sets. We can observe that DICE measures are withing 0.83 and 0.97 and the majority of the resulting PVE values are negative, implying that they were over segmented. The average value of the DICE coefficient and PVE is 0.94 and -4.86% respectively. Fig. 3 illustrates a 2D axial and coronal view of the obtained results, while Fig. 4 depicts the final 3D liver volume classified following Couinaud's scheme with different colors representing the different segments.

TABLE I. COMPARISON OF LIVER VOLUME SEGMENTATION BY OUR ALGORITHM TO THE GROUND TRUTH

Subject	*DICE*	*PVE (%)*	*FP (%)*	*FN (%)*
1	0.94	-7.60	0.10	1.78
2	0.96	-3.98	0.86	0.81
3	0.96	-6.37	0.56	0.75
4	0.96	4.83	3.15	0.22
5	0.95	-8.62	0.41	1.50
6	0.96	0.37	2.18	0.51
7	0.91	0.37	4.38	1.05
8	0.95	-1.73	2.10	1.19
9	0.95	-1.78	1.97	0.82
10	0.97	-4.63	0.52	1.04
11	0.96	-5.25	0.47	0.58
12	0.83	-34.04	0.44	6.37
13	0.96	-4.47	0.93	0.87
14	0.95	-5.41	1.35	1.18
15	0.96	-3.91	1.07	0.98
16	0.94	-6.73	1.17	1.31
17	0.95	-3.72	1.52	0.94
18	0.94	-7.19	1.27	1.68
19	0.92	-5.41	1.44	1.09
20	0.94	8.13	5.09	0.35
Average	**0.94**	**-4.86**	**1.09**	**0.97**
Standard deviation	**± 0.03**	**± 8.03**	**± 1.32**	**± 1.27**

It can be noted that subject 12 obtained a significantly lower DICE coefficient. This is due to the presence of a large sized tumour that leads to a deformation of the anatomical shape of the liver and thus, to a high shape variability between this subject and the models used as atlas for the segmentation. Furthermore, the high PVE (-34.04%) obtained for this subject

indicates that a 0.8 threshold is too high as it leaves out a high number of pixels that belong to liver tissue.

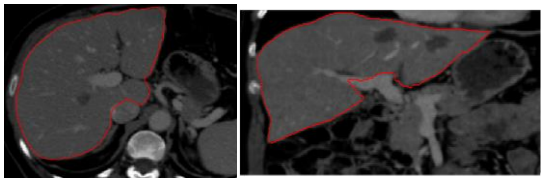

Fig. 3 Axial (a) and coronal (b) view of segmentation results for IRCAD subject 10.

Even so, good scores where achieved for liver segmentation on subjects with a high anatomical and pathological variability, obtaining an excellent average value of the DICE coefficient of 0.94.

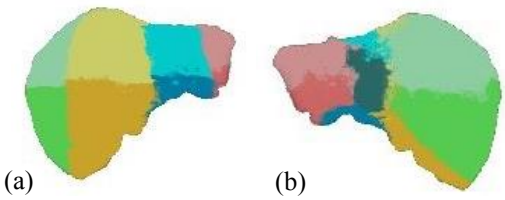

(a) (b)

Fig. 4 (a) and (b) depict two different views of the 3D display of the resulting liver segments according to Couinaud's scheme. S.I (dark blue), S.II (light pink), SIII (pink), S.IVa (light blue), IVb (blue) V(light yellow), S.VI (yellow), S.VII (light green), S.VIII (green).

Finally, our method also classifies the liver volume automatically into the 8 Couinaud segments based on the labels of the SPL Liver atlas.

IV. Conclusion

In clinical hepatectomy planning and surgical intervention, the segmentation and classification of the liver based on the Couinaud segments are a crucial step. This works presents the development and implementation of an atlas-based segmentation algorithm that provides an automatic segmentation of the liver volume and its Couinaud-based classification. This algorithm has been tested in 20 CT volumes from men and women with high variability regarding size and location of hepatic tumors. The results were compared to the ground truth and show that multi-atlas-based segmentation can offer around 94% accuracy on liver segmentation. The next stage of this work would be to obtain multiple atlas with Couinaud labels included to execute multi-atlas-based classification of liver volume.

References

[1] Valery, P.C., Laversanne, M., Clark, P.J., Petrick, J.L., McGlynn, K.A. and Bray, F., 2018. Projections of primary liver cancer to 2030 in 30 countries worldwide. Hepatology, 67(2), pp.600-611.

[2] Orcutt, S.T. and Anaya, D.A., 2018. Liver resection and surgical strategies for management of primary liver cancer. Cancer Control, 25(1), p.1073274817744621.

[3] Couinaud C., 1999. Liver anatomy: portal (and suprahepatic) or biliary segmentation. Digestive surgery 16(6):459-67.

[4] Alirr, O.I. and Rahni, A.A.A., 2020. Automatic atlas-based liver segmental anatomy identification for hepatic surgical planning. International Journal of Computer Assisted Radiology and Surgery, 15(2), pp.239-248.

[5] Vanmore, S.V. and Chougule, S.R., 2019, May. Survey on Automatic Liver Segmentation Techniques from Abdominal CT Images. In 2019 International Conference on Intelligent Computing and Control Systems (ICCS) (pp. 1030-1035). IEEE.

[6] Platero, C. and Tobar, M.C., 2014. A multiatlas segmentation using graph cuts with applications to liver segmentation in CT scans. Computational and mathematical methods in medicine, 182909.

[7] Gotra, A., Sivakumaran, L., Chartrand, G., Vu, K.N., Vandenbroucke-Menu, F., Kauffmann, C., Kadoury, S., Gallix, B., de Guise, J.A. and Tang, A., 2017. Liver segmentation: indications, techniques and future directions. Insights into imaging, 8(4), pp.377-392.

[8] Eapen, M., Korah, R. and Geetha, G., 2015. Swarm intelligence integrated graph-cut for liver segmentation from 3D-CT volumes. The Scientific World Journal, 2015.

[9] Qiao, S., Xia, Y., Zhi, J., Xie, X. and Ye, Q., 2020, June. Automatic liver segmentation method based on improved region growing algorithm. In 2020 IEEE 4th Information Technology, Networking, Electronic and Automation Control Conference (ITNEC) (Vol. 1, pp. 644-650). IEEE

[10] Zhou, Z., Xue-chang, Z., Si-ming, Z., Hua-fei, X. and Yue-ding, S., 2018. Semi-automatic Liver Segmentation in CT Images Through Intensity Separation and Region Growing. Procedia computer science, 131, pp.220-225

[11] Alirr, O.I. and Rahni, A.A., 2018. Automatic liver segmentation from ct scans using intensity analysis and level-set active contours. J Eng Sci Technol, 13(11), pp.3821-3839.

[12] Platero, C. and Tobar, M.C., 2014. A multiatlas segmentation using graph cuts with applications to liver segmentation in CT scans. Computational and mathematical methods in medicine, 2014.

[13] Rafiei, S., Karimi, N., Mirmahboub, B., Najarian, K., Felfeliyan, B., Samavi, S. and Soroushmehr, S.R., 2019, July. Liver Segmentation in Abdominal CT Images Using Probabilistic Atlas and Adaptive 3D Region Growing. In 2019 41st Annual International Conference of the IEEE Engineering in Medicine and Biology Society (EMBC) (pp. 6310-6313). IEEE.

[14] Lu, X., Xie, Q., Zha, Y. and Wang, D., 2018. Fully automatic liver segmentation combining multi-dimensional graph cut with shape information in 3D CT images. Scientific reports, 8(1), pp.1-9.

[15] Rohlfing, T., Brandt, R., Menzel, R., Russakoff, D.B. and Maurer, C.R., 2005. Quo vadis, atlas-based segmentation?. In Handbook of biomedical image analysis (pp. 435-486). Springer, Boston, MA.

[16] Dice, L.R., 1945. Measures of the amount of ecologic association between species. Ecology, 26(3), pp.297-302.

[17] Klein, S., Staring, M., Murphy, K., Viergever, M.A. and Pluim, J.P., 2009. Elastix: a toolbox for intensity-based medical image registration. IEEE transactions on medical imaging, 29(1), pp.196-205

[18] Iglesias, J.E. and Sabuncu, M.R., 2015. Multi-atlas segmentation of biomedical images: a survey. Medical image analysis, 24(1), pp.205-219.